Asymmetry in the Duration of El Niño and La Niña

YUKO M. OKUMURA AND CLARA DESER

Climate and Global Dynamics Division, National Center for Atmospheric Research, Boulder, Colorado

(Manuscript received 22 December 2009, in final form 10 May 2010)

ABSTRACT

El Niño and La Niña are not a simple mirror image, but exhibit significant differences in their spatial structure and seasonal evolution. In particular, sea surface temperature (SST) anomalies over the equatorial Pacific cold tongue are larger in magnitude during El Niño compared to La Niña, resulting in positive skewness of interannual SST variations. The associated atmospheric deep convection anomalies are displaced eastward during El Niño compared to La Niña because of the nonlinear atmospheric response to SST. In addition to these well-known features, an analysis of observational data for the past century shows that there is a robust asymmetry in the duration of El Niño and La Niña. Most El Niños and La Niñas develop in late boreal spring/summer, when the climatological cold tongue is intensifying, and they peak near the end of the calendar year. After the mature phase, El Niños tend to decay rapidly by next summer, but many La Niñas persist through the following year and often reintensify in the subsequent winter. Throughout the analysis period, this asymmetric feature is evident for strong events in which Niño-3.4 SST anomalies exceed one standard deviation in December. Seasonally stratified composite analysis suggests that the eastward displacement of atmospheric deep convection anomalies during El Niño enables surface winds in the western equatorial Pacific to be more affected by remote forcing from the Indian Ocean, which acts to terminate the Pacific events.

1. Introduction

In the equatorial Pacific, prevailing easterly winds accumulate warm surface water to the west, lifting the thermocline in the east. The equatorial upwelling forced by these easterly winds induces stronger surface cooling in the eastern Pacific because of the shallower thermocline. The resulting zonal gradient of sea surface temperature (SST), in turn, drives the equatorial easterly winds that gather water vapor to fuel intense atmospheric deep convection over the western Pacific warm pool. Weakened (strengthened) easterly winds reduce (enhance) the eastern cooling and hence the zonal SST gradient, which positively feeds back to the surface wind changes. This so-called Bjerknes (1969) feedback is at the heart of interannual tropical Pacific variability, the El Niño–Southern Oscillation (ENSO) phenomenon, whose impact extends far beyond the tropical Pacific through global atmospheric teleconnections (e.g., Trenberth et al. 1998; Alexander et al. 2002). Warm (El Niño) and cold (La Niña) ENSO events tend to last approximately 1–2 years and recur every 3–8 years.

Various theories have been proposed to explain what brings turnabouts between El Niño and La Niña, including ocean wave reflection at the western boundary (Schopf and Suarez 1988; Battisti and Hirst 1989), recharge/discharge of warm water volume due to Sverdrup transport (Jin 1997), oceanic Kelvin waves forced by wind anomalies in the western Pacific (Weisberg and Wang 1997), and ocean temperature advection by zonal currents associated with wave reflection at the western and eastern boundaries (Picaut et al. 1997). [See Neelin et al. (1998), Wang and Picaut (2004), and Chang et al. (2006) for reviews of ENSO mechanisms.] Despite their differences, these theories agree that dynamical oceanic adjustments provide a slow restoring force to the unstable equatorial air–sea interactions. Irregularity and noncyclic behavior of ENSO have also led some authors to propose that ENSO is not a self-sustained oscillatory mode but a stable mode triggered by stochastic wind forcing (e.g., Lau 1985; Penland and Sardeshmukh 1995; Thompson and Battisti 2001; Kessler 2002).

El Niño and La Niña are strongly modified by the background seasonal cycle. In particular, the equatorial

Corresponding author address: Dr. Yuko M. Okumura, Climate and Global Dynamics Division, NCAR, P.O. Box 3000, Boulder, CO 80307.
E-mail: yukoo@ucar.edu

DOI: 10.1175/2010JCLI3592.1

Pacific cold tongue exhibits a distinct annual variation despite the semiannual solar forcing (Mitchell and Wallace 1992; Xie 1994). The associated zonal SST gradient across the equatorial Pacific and accompanying easterly winds are strongest (weakest) in boreal summer–fall (spring) when the intertropical convergence zone (ITCZ) moves farthest from (closest to) the equator. (In this paper the seasons refer to those in the Northern Hemisphere.) Both El Niño and La Niña develop in late spring–summer, when the climatological cold tongue is intensifying, and they peak mostly toward the end of the calendar year, resulting in a December peak in monthly SST anomaly variance. The physical processes responsible for this phase locking are still unclear but possibilities include nonlinear modulation of the annual cycle by interannual displacement of the thermocline (Xie 1995), seasonal migration of the ITCZ and associated atmospheric heating (Tziperman et al. 1997; Harrison and Vecchi 1999), delayed negative feedback from the Indian Ocean (Annamalai et al. 2005; Kug and Kang 2006; Ohba and Ueda 2007; Yoo et al. 2010), and influence of the North Pacific Oscillation (Chang et al. 2007; Alexander et al. 2010). The fact that both El Niño and La Niña amplify during the equatorial cold season confirms that the presence of strong zonal SST gradient, easterly winds, and upwelling in the background state is fundamental for the Bjerknes feedback.

Historically, El Niño has drawn more attention than La Niña, partly because it is associated with more severe climatic conditions, such as heavy rains in the coastal desert of Peru and sometimes failures of the Indian monsoon. In fact, composite analysis had only been attempted for El Niño and not for La Niña until the late 1980s. After the cold phase of ENSO was named ''La Niña'' by Philander (1985) and its climatic impact caught public attention with one of the strongest events on record in 1988–89 (e.g., Kerr 1988), researchers began to treat El Niño and La Niña as complementary phases of ENSO. Indeed, most observational studies use linear techniques such as regression analysis, empirical orthogonal function (EOF) analysis, or warm-minus-cold composites to identify the canonical patterns and evolution of ENSO events, assuming that La Niña is a mirror image of El Niño.

Interannual SST variations along the coast of Peru are known to be strongly positively skewed (Deser and Wallace 1987). Burgers and Stephenson (1999) show that the SST anomaly skewness exhibits an intriguing geographical distribution, with large positive values in the eastern equatorial Pacific and small negative values in the western Pacific, reflecting that the SST anomalies associated with El Niño are larger in magnitude than those associated with La Niña. This deviation from normality led them to question the degree of linearity in the equatorial Pacific ocean–atmosphere system. They suggest that the proximity of the thermocline to the surface is the cause for the positive SST anomaly skewness in the eastern equatorial Pacific, and that therefore nonlinear oceanic processes are responsible for the asymmetry in the strength of El Niño and La Niña. Jin et al. (2003) propose that nonlinear thermal advection by ocean currents contributes to the generation of larger-amplitude El Niños compared to La Niñas. Meinen and McPhaden (2000) show that for a given anomaly magnitude of warm water volume in the upper portion of the equatorial Pacific, positive values are associated with larger-amplitude SST anomalies than negative values, suggesting the importance of nonlinear processes.

Asymmetry in the spatial distribution of equatorial Pacific rainfall anomalies between El Niño and La Niña was highlighted in the study of Hoerling et al. (1997) on ENSO teleconnections. They noted that maximum amplitude rainfall anomalies along the equator are located east (west) of the date line during El Niño (La Niña), with a commensurate shift (approximately 35° of longitude) in the atmospheric Rossby wave trains forced by diabatic heating changes. Hoerling et al. (1997) suggested that the zonal displacement is due to the nonlinear dependence of atmospheric deep convection on total SSTs. On the periphery of the warm pool, even small SST deviations excite large rainfall deviations because of the high background SST values. Thus, maximum convection anomalies are shifted more than 5000 km west of the maximum SST anomalies (Deser and Wallace 1990). Over the eastern cold tongue region, on the other hand, large positive SST anomalies can induce convection while negative anomalies have no further effect on the normally dry conditions. Indeed, an atmospheric general circulation model (GCM) forced with perfectly symmetric positive and negative SST anomaly patterns successfully simulates the nonlinear atmospheric response that closely resembles the observed patterns (Hoerling et al. 1997). The associated zonal shift of surface wind anomalies, in turn, is suggested to cause stronger positive SST anomalies in the eastern Pacific during El Niño (Kang and Kug 2002).

Thus, the asymmetry of El Niño and La Niña involves nonlinear processes in both the ocean and atmosphere, which may be amplified by air–sea interactions. An alternative linear view is that ENSO represents zonal excursions of the ocean temperature front between the western warm pool and the eastern cold tongue by anomalous advection: its eastward (westward) displacement results in large positive (negative) SST anomalies to the east (west) of the climatological front (Schopf and Burgman 2006). Previous studies of ENSO asymmetry have focused on the skewness of SST anomalies and its spatial pattern. It

should be noted that this asymmetry in the magnitude of positive and negative SST anomalies may also arise from the asymmetry in the duration of warm and cold phases of ENSO when climatologies are defined as the time mean state.

The asymmetry in the duration of El Niño and La Niña has been noted in a few recent studies (Larkin and Harrison 2002; McPhaden and Zhang 2009; Ohba and Ueda 2009). McPhaden and Zhang (2009) show that La Niña tends to persist into the second year and reintensify in winter in their composite analysis for 1980–2008, although this feature is not evident for the earlier period 1950–77. For both periods, El Niño tends to terminate rapidly after the mature phase, as shown in earlier studies by Rasmusson and Carpenter (1982) and others. Based on the observational analysis for 1980–2002, Kessler (2002) also points out that the transitions from La Niña to El Niño are slower than those from El Niño to La Niña. Ohba and Ueda (2009) suggest that these asymmetric transitions between El Niño and La Niña can be attributed to the nonlinear response of surface winds to Indo-Pacific SST anomalies, although they did not clarify the relative role of the Indian Ocean SST anomalies associated with ENSO.

In the present study, we examine in greater detail the asymmetry in the duration of El Niño and La Niña, using a suite of observational and reanalysis datasets spanning the past 27–109 yr. We address the following questions. Is there a robust asymmetry in the duration of the two ENSO phases throughout the observational record? How do ocean–atmosphere anomalies evolve in association with the asymmetric duration of El Niño and La Niña, and what causes this asymmetric evolution? Do SST changes in the Indian Ocean associated with El Niño and La Niña have any impact on the asymmetric wind anomalies in the Pacific? These are very important issues for climate prediction because long-lasting La Niña can exert persistent climatic impact on the Indo-Pacific and distant regions through atmospheric teleconnections (e.g., Ropelewski and Halpert 1989; Cole et al. 2002; Hoerling and Kumar 2003).

The datasets and analysis methods used in this study are described in section 2. In section 3, it is shown that there is a robust asymmetry in the duration of the two ENSO phases throughout the past century, especially for strong events. Through seasonally stratified composite analysis, we identify a pronounced asymmetry in the surface wind anomalies that develop in late fall over the far western Pacific, leading to the asymmetric evolution of thermocline anomalies in the central-eastern portion of the basin in the following seasons. We discuss a possible role for the Indian Ocean in this asymmetric evolution of surface wind anomalies over the far western Pacific. The last section summarizes the main results.

2. Data and methods

To identify any robust asymmetry in the duration of El Niño and La Niña, we analyze two monthly SST datasets spanning different periods: the Hadley Centre sea ice and sea surface temperature (HadISST; Rayner et al. 2003) for 1900–2008 and the National Oceanic and Atmospheric Administration (NOAA) optimum interpolation sea surface temperature version 2 (OISST; Reynolds et al. 2002) for 1982–2008. The HadISST is a long-term global SST analysis available on a 1° grid from 1870 to the present. It is based on historical in situ ship and buoy observations with satellite data blended in after 1982. The cold bias of bucket SST measurements prior to 1942 is corrected for, and missing grids are filled by optimal interpolation based on EOF analysis. The OISST combines satellite data with in situ observations and is available on a 1° grid from December 1981 to the present. The long, spatially complete data of HadISST helps us assess the robustness of asymmetry throughout the historical record, while the extensive spatiotemporal coverage of satellite observations used in the OISST allows for better resolution of SST variations with small amplitude and spatial scale (e.g., Okumura and Xie 2006).

Several other monthly ocean–atmosphere variables are analyzed in conjunction with the SST field: surface wind velocities and tropospheric air temperature from the National Centers for Environmental Prediction–National Center for Atmospheric Research (NCEP–NCAR) reanalysis for 1948–2008 (Kalnay et al. 1996) and from the NCEP–Department of Energy (DOE) reanalysis II for 1979–2008 (Kanamitsu et al. 2002), precipitation from the Climate Prediction Center Merged Analysis of Precipitation (CMAP) for 1979–2008 (Xie and Arkin 1996), and sea surface height and surface wind stress from the Simple Ocean Data Assimilation (SODA) analysis versions 2.0.2 and 2.0.4 for 1958–2001 and 2002–2007, respectively [see Carton and Giese (2008) for the description of the earlier version]. It should be noted that a representation of the Pacific ITCZ and associated meridional winds is substantially improved in the NCEP–DOE reanalysis II compared to the original NCEP–NCAR reanalysis presumably due to improved model physics of boundary layer and convection (Wu and Xie 2003). The two versions of the SODA analysis use different wind products (the European Centre for Medium-Range Weather Forecasts reanalysis in version 2.0.2 and the Quick Scatterometer data in version 2.0.4) but do not exhibit any apparent discontinuity in the equatorial Pacific across the two periods, and thus we merge them to form a single record for 1958–2007. The results shown in the following section do not change significantly by limiting the data period to 1958–2001.

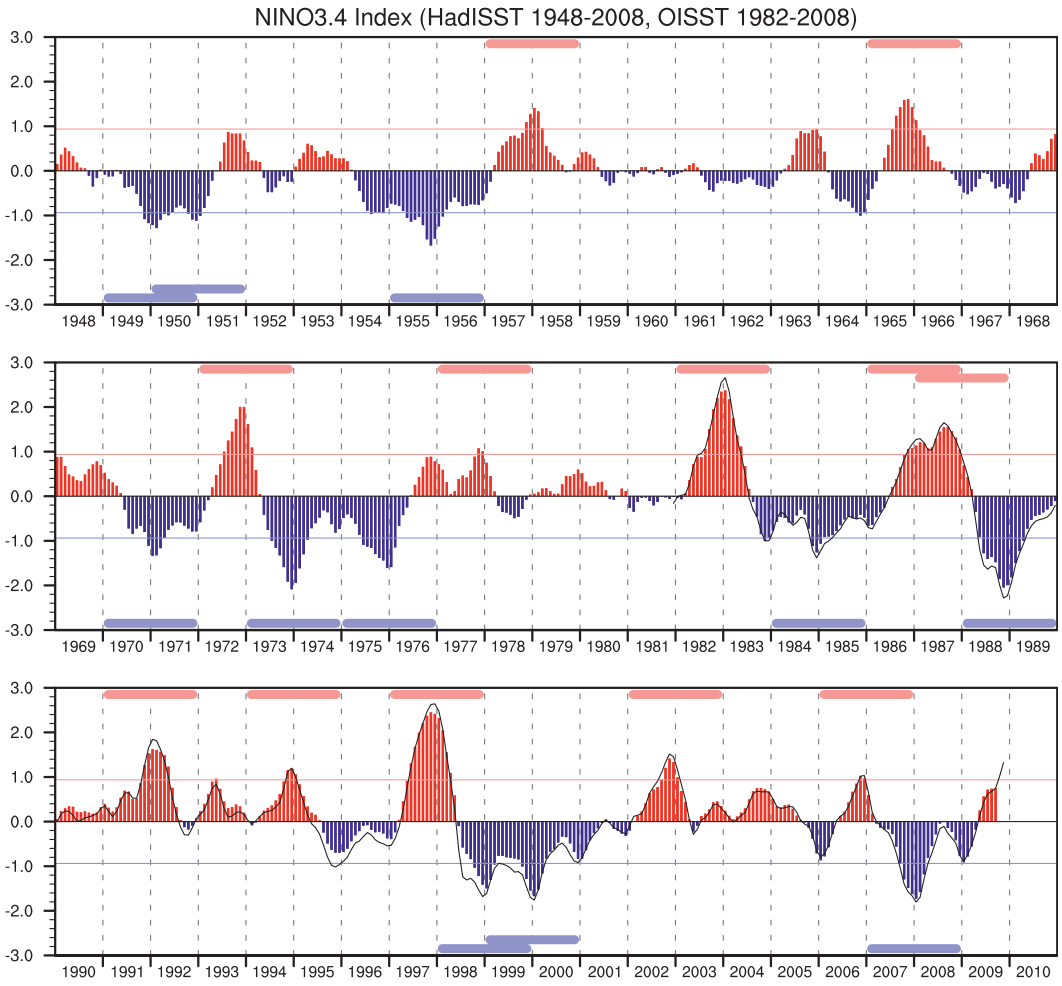

FIG. 1. Time series of the Niño-3.4 index based on the HadISST for 1948–2008 (color bars) and the OISST for 1982–2008 (black line). El Niño and La Niña years are marked from Jan^{0} to Dec^{+1} by thick horizontal red and blue bars, respectively. Thin horizontal color lines indicate one standard deviation of the Niño-3.4 index in December based on the HadISST (0.94). Both the HadISST Niño-3.4 index and its standard deviation are calculated for the base period 1900–2008.

For each variable, monthly anomalies are calculated by subtracting the climatological monthly means over the analysis period. When two or more variables are analyzed together, a common data period is used to calculate the climatologies. The monthly anomalies are smoothed using a 1–2–1 filter. We choose not to remove linear trends from the data records since they are not consistent for the different data periods and may arise from interdecadal variability in the short records spanning the recent few decades. The SST trend in the central-eastern equatorial Pacific is small over the past century relative to the amplitude of El Niño and La Niña (~±0.2°C). Although the tropical Indian Ocean shows a significant warming trend of ~1.0°C from 1900 to 2008, we confirm that it does not significantly affect the composite anomalies for El Niño and La Niña.

As will be shown in the next section, the asymmetry in the duration of El Niño and La Niña is evident only for strong events. Based on the fact that most strong ENSO events peak toward the end of the year, El Niño and La Niña years are defined as those for which the 1–2–1 smoothed SST anomalies averaged over the Niño-3.4 region (5°S–5°N, 120°–170°W, hereafter called the Niño-3.4 index; Fig. 1) in December exceed 1 standard deviation and are below −1 standard deviation, respectively. This method picks out all strong cases of El Niño and La Niña events according to the definition of Trenberth (1997) that is used in NOAA's operational ENSO forecast and many previous studies. Composite analysis is conducted for these El Niño and La Niña years separately. The El Niño/La Niña and subsequent years are denoted as "year 0," "year +1," . . . and the months of these years as

TABLE 1. El Niño and La Niña years defined according to the HadISST for 1900–2008. In December of these years the absolute value of the Niño-3.4 index exceeds one standard deviation (0.94). The set of years used in the composites based on the HadISST for 1900–47 (the HadISST and NCEP–NCAR reanalysis for 1948–2008) are listed in the first (second) row. The set of years used in the composites based on the OISST, NCEP–DOE reanalysis II, and CMAP for 1982–2008 are set bold.

El Niño years	1902, 1905, 1911, 1918, 1925, 1930, 1940, 1941, 1957, 1965, 1972, 1977, **1982, 1986, 1987, 1991, 1994, 1997, 2002, 2006**
La Niña years	1909, 1916, 1933, 1942, 1949, 1950, 1955, 1970, 1973, 1975, **1984, 1988, 1998, 1999, 2007**

"Jan^0", "Feb^0," ... "Jan^{+1}," "Feb^{+1}," etc. We use the HadISST to define El Niño and La Niña years for 1900–2008 (Table 1). Twelve El Niños and 11 La Niñas are identified for the period 1948–2008, and are indicated by horizontal bars from Jan^0 through Dec^{+1} on the Niño-3.4 time series shown in Fig. 1. There are several cases in which the absolute value of the Niño-3.4 index exceeds one standard deviation in December of two consecutive years due to persistent warm or cold conditions (1940/41, 1949/50, 1986/87, and 1998/99). These consecutive El Niño and La Niña years are regarded as single events in Trenberth's (1997) definition, but are treated as separate samples in our composite analysis because we are interested in how the ocean–atmosphere anomalies evolve before and after each peak of equatorial SST anomalies. The results shown in the following section are, however, not significantly affected by eliminating the second years from the analyses. The main results also do not change for slight modifications of the year selection criteria (e.g., expanding the reference months to include November and January) or by excluding the two extreme El Niños of 1982/83 and 1997/98 in the composite.

3. Results

a. Duration of El Niño and La Niña

The long-lasting La Niña of 1998–2001 caused extensive drought across the United States, southern Europe, and southwest Asia (e.g., Hoerling and Kumar 2003). An examination of the Niño-3.4 index time series for 1948–2008 reveals many other strong, persistent cold phases spanning more than 2 yr (1949–51, 1954–56, 1973–76, 1983–86, and 2007–09; Fig. 1). During these persistent cold phases, negative SST anomalies reintensify each winter, evidenced by the sawtooth shape of the Niño-3.4 time series. Although there were two prolonged warm phases during this period (1990–95 and 2002–05), none was as continuously strong as their cold counterparts. Indeed, there is no warm phase in which the Niño-3.4 index remains above 0.3–0.4 for more than 2 yr. In 9 out of 11 La Niñas the Niño-3.4 index remained negative through year +1, while 11 out of 12 El Niños terminated rapidly by summer of year +1. The three major El Niños of 1972/73, 1982/83, and 1997/98 were followed by a strong, persistent cold phase.

Figure 2 shows the temporal evolution of the Niño-3.4 index for the composite El Niño (top) and La Niña (bottom) as well as for the individual years that comprise the composites. In the composite La Niña, negative values of the Niño-3.4 index persist for more than 22 months (Mar^0–Dec^{+1}), but in the composite El Niño positive values last for only 15 months (Mar^0–May^{+1}). In the second half of year +1, the Niño-3.4 indices for the composite El Niño and La Niña have the same sign and similar magnitudes. Most of the strong El Niños and La Niñas that compose the composites develop in late spring. Horii and Hanawa (2004) have pointed out that warm events that commence in spring tend to grow larger and exhibit a more regular life cycle than those that commence in summer–fall. The El Niño of 1986–87 did not begin until late summer and lasted through year +1 as many of the summer–fall-type events in Horii and Hanawa's (2004) analysis. The El Niño of 2006/07 also began in late summer but terminated rapidly after the mature phase, triggered by intraseasonal variability emanating from the Indian Ocean (McPhaden 2008).

An expanded view of the composite evolution of SST anomalies along the equator during El Niño and La Niña is shown in Fig. 3 for three different periods and two datasets: 1900–47 (HadISST), 1948–2008 (HadISST), and 1982–2008 (OISST). For the periods after 1948, composite surface wind anomalies are also overlaid. The greater persistence of La Niña compared to El Niño is apparent in all three periods and two datasets. In the composite El Niño, positive SST anomalies are replaced by negative SST anomalies starting in summer of year +1, accompanied by a reversal of the zonal wind anomalies west of 170°W. In the composite La Niña, on the other hand, negative SST anomalies persist through year +1 in the western-central Pacific and reintensify in winter. The persistent negative SST anomalies in the western-central Pacific are associated with persistent easterly wind anomalies west of 170°W, which would increase local upwelling and force upwelling Kelvin waves to the east. To the east of 145°W, the negative SST anomalies weaken significantly after the mature phase and then reintensify in the following fall–winter. In the La Niña composite

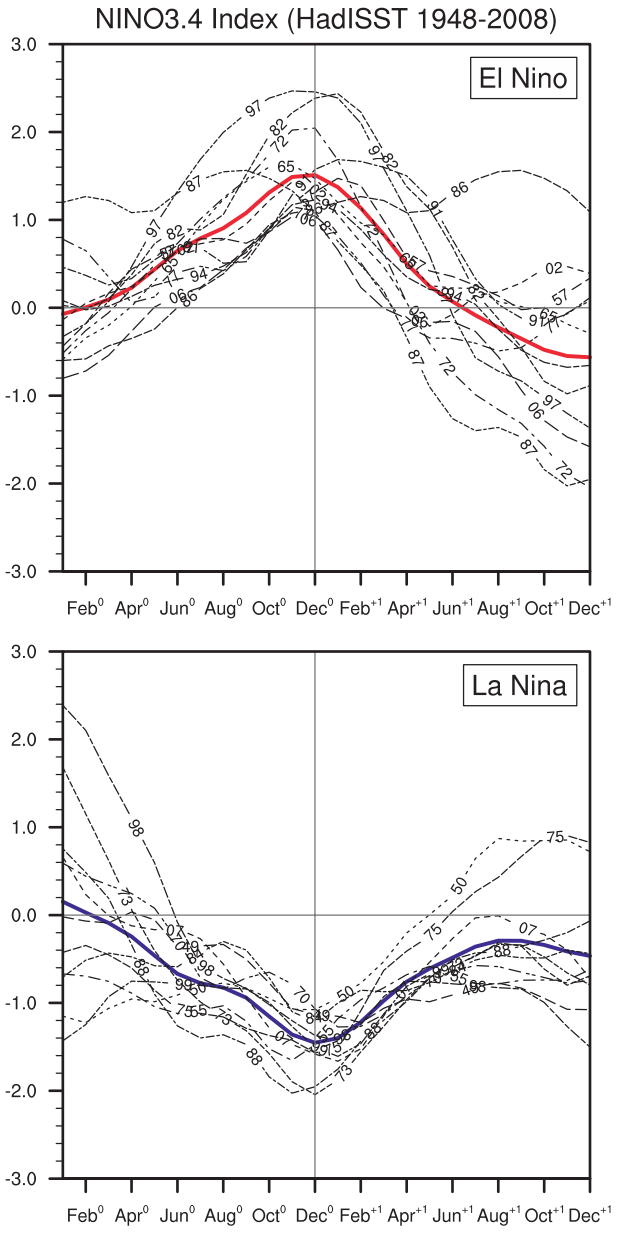

FIG. 2. Time series of the Niño-3.4 index overlaid from Jan^{0} to Dec^{+1} for (top) El Niño and (bottom) La Niña during 1948–2008 based on the HadISST. Thick red and blue lines are composite time series.

based on the OISST and NCEP–DOE reanalysis II, this decay of negative SST anomalies in the eastern Pacific is associated with anomalous westerly winds that intensify east of 120°W after the mature phase, which would reduce local upwelling and warm the ocean mixed layer (Zhang and McPhaden 2006, 2008). As described in previous studies, asymmetry is also found in the longitudinal structure of SST and wind anomalies. During the mature phase, the positive SST anomalies associated with El Niño are larger than the negative SST anomalies associated with La Niña east of 100°–110°W although this asymmetric feature is less pronounced in the early part of the record (1900–47). Compared to the positive SST anomalies associated with El Niño, the negative SST anomalies associated with La Niña extend farther west by approximately 10° of longitude in the western Pacific. The associated wind anomalies are also shifted westward in La Niña compared to El Niño.

The Hovmöller plots in Fig. 3 reveal several other interesting features consistent for different periods and datasets. During year 0 of the composite La Niña, negative SST anomalies expand westward from the eastern Pacific. A similar westward propagation is evident for the negative SST anomalies that develop in year +1 of the composite El Niño. In contrast, the reintensification of the negative SST anomalies toward the end of year +1 of the composite La Niña occurs simultaneously across the basin. The positive SST anomalies associated with the composite El Niño show a westward propagation similar to that seen for La Niña in the early part of the record (1900–47). However, there is almost no westward movement during the later portion of the record (1948–2008 and 1982–2008) for El Niño, in contrast to La Niña. Composites for different epochs of Pacific interdecadal variability suggest that they tend to propagate westward (eastward) during cold (warm) epochs of the Indo-Pacific region (not shown), consistent with earlier studies that suggest that the propagation characteristics of ENSO changed after the Pacific-wide climate regime shift in late 1970s (e.g., Fedorov and Philander 2000; Wang and An 2002; Trenberth et al. 2002). McPhaden and Zhang (2009) discuss the asymmetry in the propagation characteristics of El Niño and La Niña, which cannot be explained by existing theories.

The time evolution of equatorial SST and wind anomalies for the two most recent persistent cold phases (1998–2001 and 2007–09) is shown in Fig. 4. These plots reveal remarkable SST and wind anomaly structures that repeat 2–4 yr in a row. The negative SST and easterly wind anomalies intensify in winter and weaken in spring–early summer. The SST anomalies reintensify in late 2008/early 2009 simultaneously across the basin, consistent with the composite La Niña (Fig. 3). However, the reintensified equatorial cooling in late 1999/early 2000 exhibits pronounced westward propagation west of 140°W, while the simultaneous reintensification across the basin occurred again in late 2000/early 2001. As in the La Niña composite based on the OISST and NCEP–DOE reanalysis II, anomalous westerly winds develop east of 140°W after the wintertime peaks of SST cooling in each year (early 1999, 2000, 2001, and 2008). In spring–summer of 2008, these anomalous westerly winds are associated with ~1°C

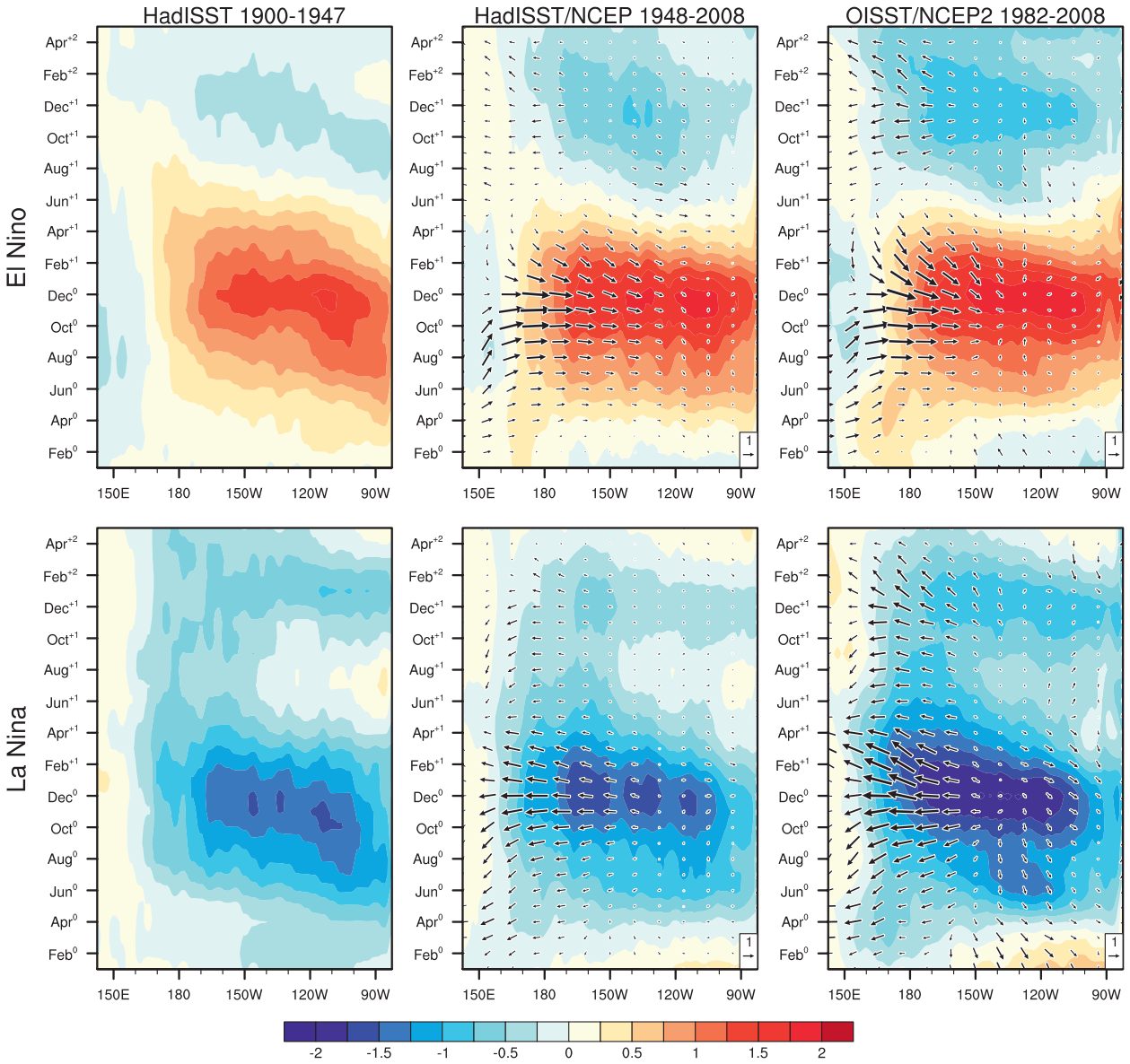

FIG. 3. Longitude–time sections of composite SST anomalies along the equator (3°S–3°N) for (top) El Niño and (bottom) La Niña, based on the HadISST for (left) 1900–47 and (middle) 1948–2008, and on the OISST for (right) 1982–2008 (°C, color shading). Composite surface wind anomalies (m s^{-1}, vectors) are overlaid in the (middle) and (right) based on the NCEP–NCAR reanalysis and the NCEP–DOE reanalysis II, respectively.

SST warming off the South American coast. The heat budget analysis by Nagura et al. (2008) for 0°, 140°W during 1998–2001, on the other hand, suggests that these anomalous westerly winds weakened the westward equatorial ocean current and hence the meridional shear between the South Equatorial Current and North Equatorial Counter Current, which in turn reduced tropical instability wave activity. The associated decrease in horizontal heat advection counteracted the warming due to a change in local upwelling, slowing down the transition from La Niña to El Niño.

b. Seasonal evolution of ocean–atmosphere anomalies in the Indo-Pacific region

Figure 5 shows bimonthly composite maps of SST, surface wind, and precipitation anomalies for El Niño and La Niña from Jun^{0} through Aug^{+1} based on the OISST, NCEP–DOE reanalysis II, and CMAP for 1982–2008. Similar SST and wind anomaly patterns are found in composites based on the HadISST and NCEP–NCAR reanalysis for 1948–2008 (not shown). In the El Niño composite, a distinct equatorial peak of SST warming

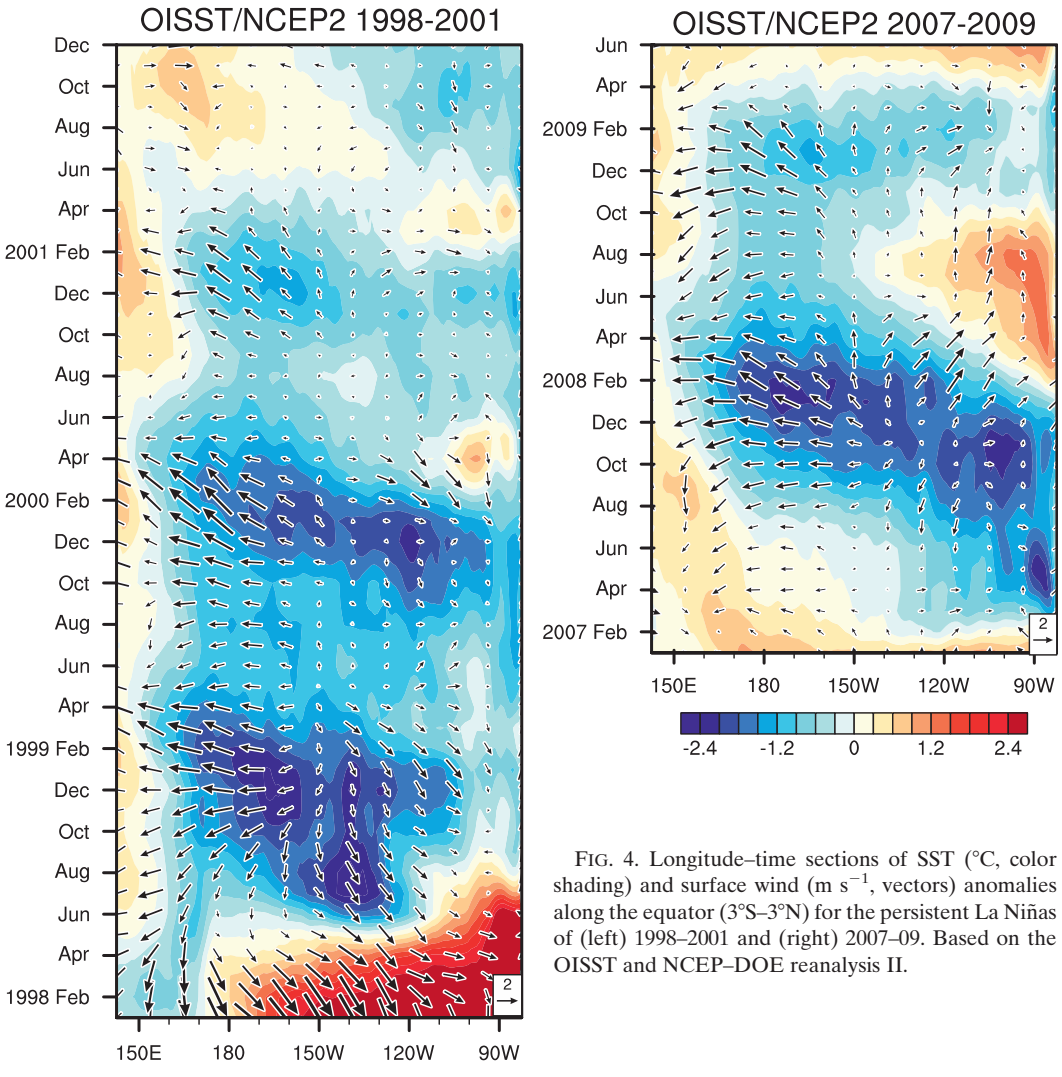

FIG. 4. Longitude–time sections of SST (°C, color shading) and surface wind (m s^{-1}, vectors) anomalies along the equator (3°S–3°N) for the persistent La Niñas of (left) 1998–2001 and (right) 2007–09. Based on the OISST and NCEP–DOE reanalysis II.

develops in the Pacific by Jun^0 and continues to intensify until Dec^0. Associated with the equatorial SST warming, precipitation increases across the equatorial Pacific and decreases over the Maritime Continent accompanied by anomalous westerly winds over the western portion of the basin. The composite La Niña exhibits a similar evolution of SST, wind, and precipitation anomalies in the Pacific throughout the developing and mature phases with the sign reversed. After the mature phase in Dec^0, the equatorial warming associated with El Niño decays rapidly and is replaced by weak equatorial cooling over the central-eastern Pacific in Jun^{+1}. The equatorial cooling, easterly wind, and negative precipitation anomalies associated with La Niña endure through the following spring-summer in the western-central Pacific.

Compared to the El Niño composite, the Pacific precipitation anomalies in the La Niña composite are displaced westward by 10°–15° in longitude and the large equatorial wind anomalies extend farther into the western Pacific throughout the developing and mature phases (Fig. 5). From Oct^0 to Dec^0 the equatorial westerly wind anomalies associated with El Niño rapidly weaken in the far western Pacific, nearly disappearing west of 160°E. The equatorial easterly wind anomalies associated with La Niña do not show such a weakening. In many strong El Niños, surface wind anomalies even become easterly in the far western Pacific after the mature phase (not shown). This wind reversal is responsible for the termination of El Niño in Weisberg and Wang's (1997) ''western Pacific oscillator'' mechanism.

After the mature phase of El Niño in Dec^0, the center of positive precipitation and westerly wind anomalies shifts south of the equator in the western-central Pacific and northerly wind anomalies appear north of the equator

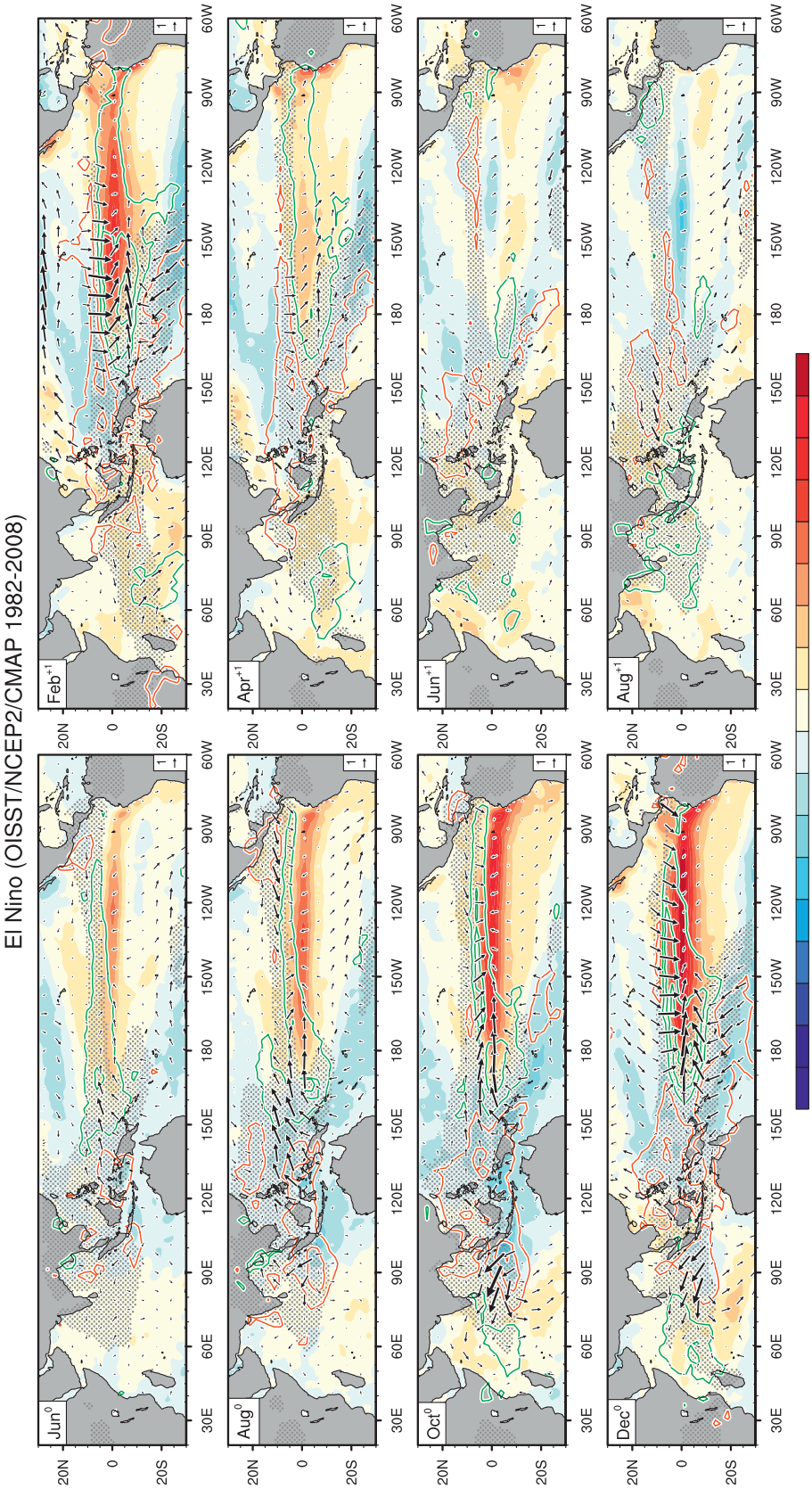

FIG. 5. Bimonthly composite maps of SST (°C, color shading), surface wind (m s^{-1}, vectors), and precipitation [mm day^{-1}, positive (negative) contours in green (orange) at ±1, 3, 5, . . .] anomalies for El Niño and La Niña from Jun^{0} to Aug^{+1}. The stippled region indicates the climatological precipitation >5 mm day^{-1}. Based on the OISST, NCEP–DOE reanalysis II, and CMAP for 1982–2008.

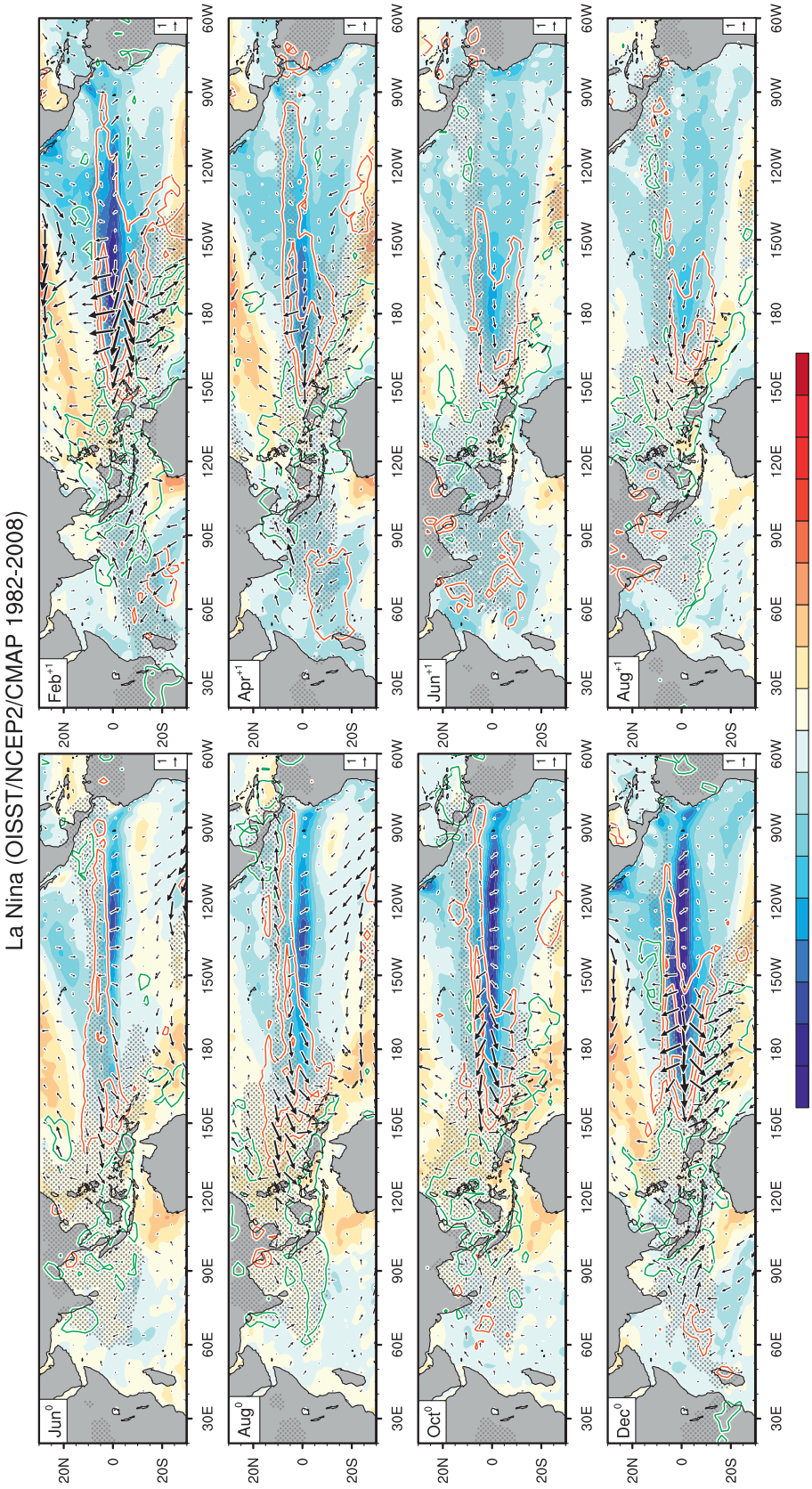

FIG. 5. (*Continued*)

(Fig. 5). Harrison and Vecchi (1999) argue that this southward wind shift hastens the termination of El Niño. Using an atmospheric GCM, Vecchi (2006) shows that the climatological seasonal movement of the western Pacific warm pool south of the equator is responsible for the southward shift of atmospheric convection and wind anomalies near the end of year. Ohba and Ueda (2009) argue that the meridional shift of the wind anomalies does not occur during the mature phase of La Niña because of the nonlinear atmospheric response to SST anomalies, prolonging the equatorial easterly wind anomalies and hence the cold phase of ENSO. Our analysis, however, shows that a similar wind shift also occurs during La Niña two months later in Feb^{+1} (Fig. 5). It is not clear why the southward wind shift during La Niña is absent in Ohba and Ueda's (2009) analysis, but it may be due to the different temporal smoothing (3-month running mean), wind product (the European Centre for Medium-Range Weather Forecasts Reanalysis), or analysis method (one-sided lag regression).

It has long been known that ENSO variability exerts a significant impact on the Indian Ocean (see Schott et al. 2009 for a recent review). In the El Niño composite, positive SST anomalies appear over the western-central tropical Indian Ocean in Jun^0 and persist through the summer of year +1 (Fig. 5). During El Niño, atmospheric deep convection is suppressed over the tropical Indian Ocean due to a change in the Walker circulation. The resulting increase in incoming solar radiation is mainly responsible for the warming of the Indian Ocean (Klein et al. 1999), with ocean dynamics also playing an important role in the southwestern part of the basin (Xie et al. 2002). In the eastern part of the basin, on the other hand, anomalous southeasterly winds associated with the suppressed convection strengthen the climatological alongshore winds and coastal upwelling off the west coast of Sumatra, inducing negative SST anomalies (Fig. 5). This zonal SST dipole is most pronounced in Oct^0 and then the eastern pole decays as the climatological winds reverse from southeasterly to northwesterly (Tokinaga and Tanimoto 2004). In Oct^0, precipitation increases over the positive SST anomalies in the western Indian Ocean, suggesting an active role of the Indian Ocean SST anomalies in modulating atmospheric circulation during El Niño (Watanabe and Jin 2002). During La Niña, the Indian Ocean exhibits a similar pattern and the evolution of ocean–atmosphere anomalies as those during El Niño with the sign reversed. Compared to the El Niño composite, the cooling of the western-central Indian Ocean is slightly weaker and delayed in the La Niña composite. The alongshore northwesterly wind anomalies and coastal SST warming off Sumatra are also weaker during Aug^0 and Oct^0 in La Niña compared to El Niño. The eastern Indian Ocean warming is more pronounced off the northwest coast of Australia and persists through the summer of year +1.

Figure 6 shows latitude–time sections of composite SST, surface wind, and precipitation anomalies averaged over the far western (140°–170°E) and western-central (170°E–150°W) Pacific. This figure confirms that the seasonal evolution of composite wind anomalies is quite symmetric between El Niño and La Niña over the western-central Pacific throughout the developing and mature phases. In the El Niño (La Niña) composite, the center of the wind anomalies shifts south of the equator in Dec^0–Jan^{+1} (Jan^{+1}–Feb^{+1}), with anomalous northerly (southerly) winds developing north of the equator. In the vicinity of the equator, the wind anomalies do not weaken prior to the mature phase. The precipitation anomalies are quite symmetric as well for El Niño and La Niña although the center south of the equator is slightly more pronounced during Dec^0–Feb^{+1} in the El Niño composite compared to the La Niña composite. In the far western Pacific (140°–170°E), on the other hand, a strong asymmetry is evident in the ocean–atmosphere anomalies (Fig. 6). During El Niño, the positive precipitation anomalies vanish by Aug^0–Sep^0 and two centers of negative precipitation anomalies develop on both sides of the equator in Oct^0–Nov^0 as the SST anomalies change from weak positive to negative. The westerly wind anomalies start to weaken in Oct^0 north of the equator and in Nov^0 in the vicinity of the equator, nearly disappearing by Jan^{+1}. During La Niña, on the other hand, the negative precipitation anomalies are about 1.5 times as large as the positive precipitation anomalies for El Niño and persist until fall of year +1. In this longitudinal band, the equatorial easterly wind anomalies continue to strengthen until Mar^{+1}. The center of the easterly wind anomalies moves north and south of the equator following the seasonal migration of the climatological rainband (e.g., north of the equator in summer–early fall and south in late winter–spring).

The composite evolution of sea surface height, surface wind stress, and SST anomalies along the equator is shown for El Niño, La Niña, and their sum in Fig. 7 based on the SODA analysis and HadISST for 1958–2007. The sea surface height anomalies, a proxy for the thermocline depth anomalies, exhibit asymmetric evolution for El Niño and La Niña similar to that of the SST anomalies. The sea surface height anomalies precede the SST anomalies by approximately one month, indicative of the subsurface influence on SSTs. During year 0 the sea surface height anomalies propagate eastward in both El Niño and La Niña in contrast to the SST anomalies that show westward (La Niña) or almost no phase propagation (El Niño). In the sum of El Niño and La Niña

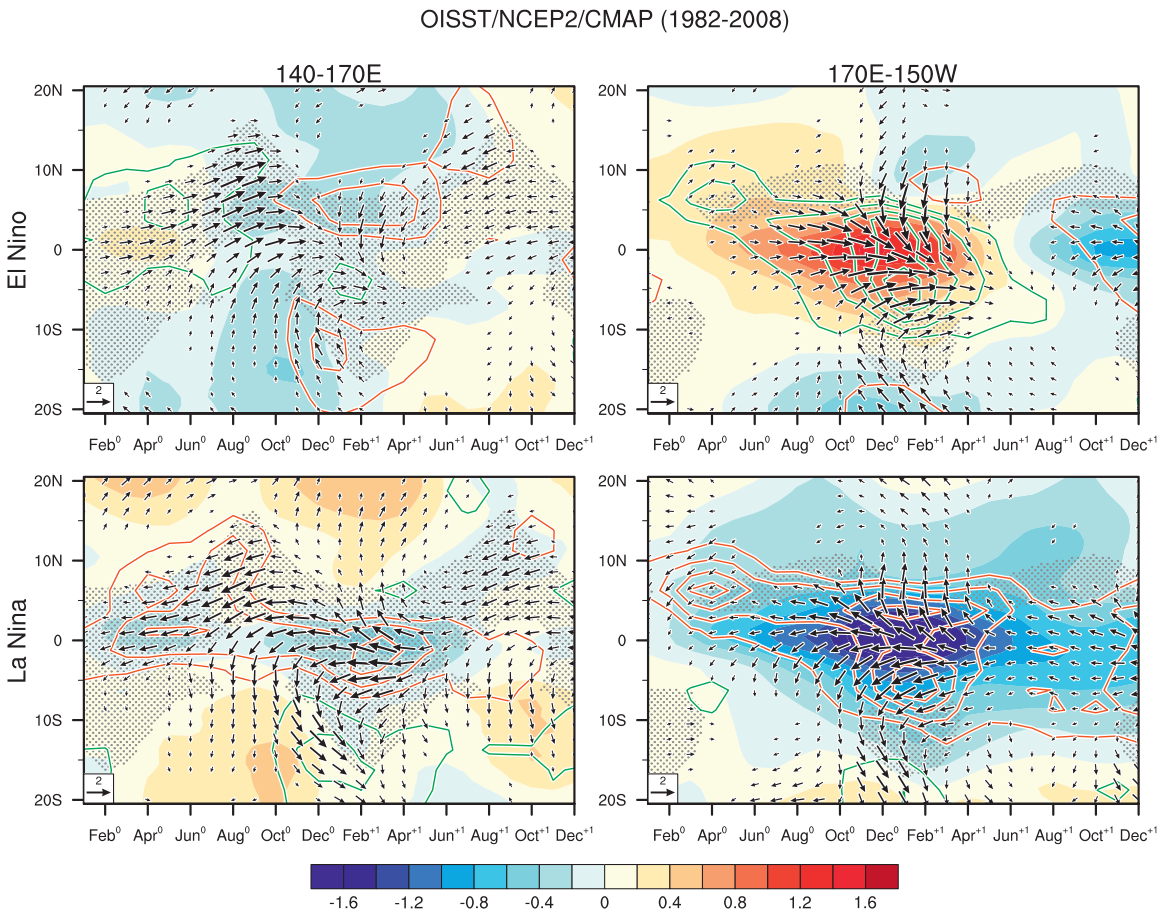

FIG. 6. Latitude–time sections of composite SST (°C, color shading), surface wind (m s^{-1}, vectors), and precipitation [mm day^{-1}, positive (negative) contours in green (orange) at intervals of 1] anomalies in (left) the far western (140°–170°E) and (right) western-central (170°E–150°W) Pacific for (top) El Niño and (bottom) La Niña. The stippled region indicates the climatological precipitation >8mm day^{-1}. Based on the OISST, NCEP–DOE reanalysis II, and CMAP for 1982–2008.

composites, easterly wind anomalies develop over the far western Pacific in Nov^0 due to the weakening of the westerly wind anomalies during El Niño. These easterly wind anomalies are associated with negative sea surface height anomalies that propagate from the western to the central-eastern Pacific in Nov^0–Feb^{+1}. These features suggest that during El Niño the weakening of the westerly wind anomalies in Nov^0 forces an upwelling oceanic equatorial Kelvin wave that rapidly terminates the equatorial warming. The timing of this wind change indicates that it is not caused by the decay of the equatorial warming but rather the other way around. Indeed, observational and modeling studies suggest that in addition to Rossby wave reflection at the western boundary, wind changes in the western Pacific force a large part of equatorial Kelvin waves that contribute substantially to the demise of El Niño in 1997/98 (McPhaden and Yu 1999; Delcroix et al. 2000; Picaut et al. 2002; Boulanger et al. 2003).

c. *Impact of the Indian Ocean SST anomalies*

Previous studies suggest that the basin warming of the tropical Indian Ocean is responsible for the weakening or reversal of equatorial westerly wind anomalies over the western Pacific at the mature phase of El Niño (Annamalai et al. 2005; Kug and Kang 2006; Ohba and Ueda 2007; Yoo et al. 2010). The Indian Ocean warming increases tropospheric temperatures by moist adiabatic adjustment in deep convection and forces a baroclinic atmospheric equatorial Kelvin wave into the Pacific. The resulting equatorial low pressure anomaly induces anomalous northeasterly winds over the northwest tropical Pacific, causing surface wind divergence and suppressed deep convection in the subtropics (Xie et al. 2009). It was shown in Fig. 5 that composite ocean–atmosphere anomalies over the Indian Ocean exhibit a similar seasonal evolution between El Niño and La Niña with the sign reversed. This raises the question, does the

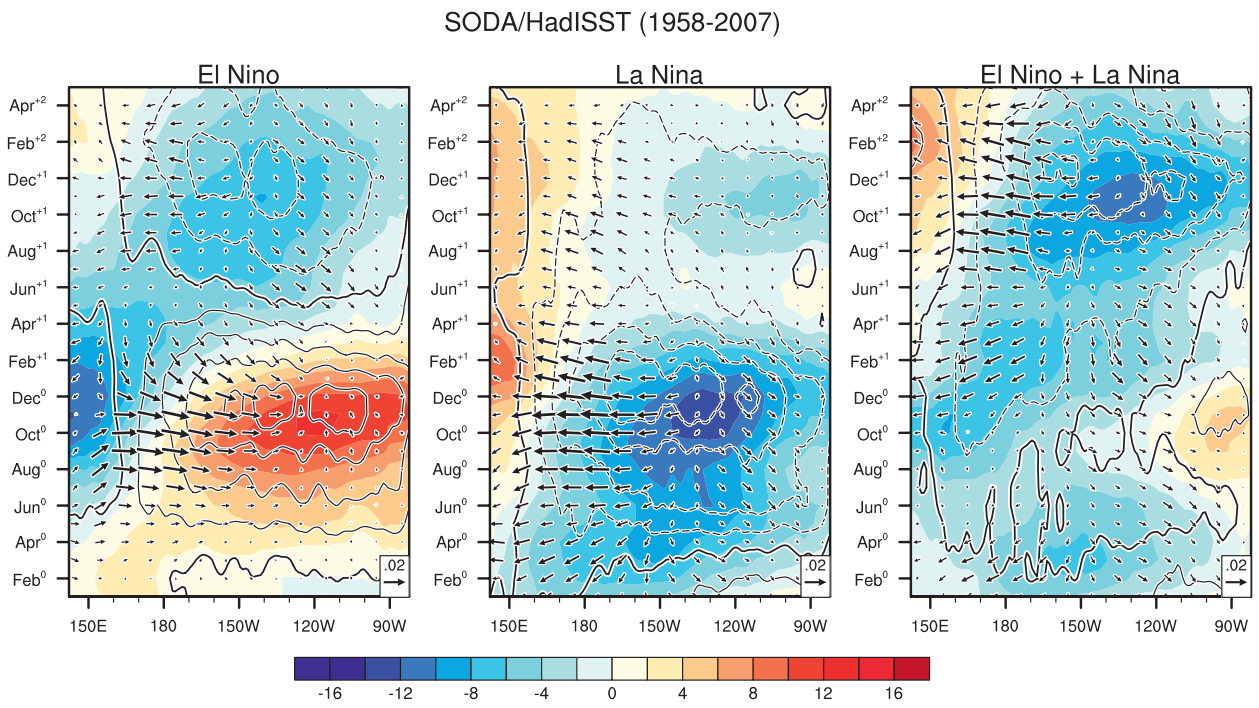

FIG. 7. Longitude–time sections of composite sea surface height (cm, color shading), surface wind stress (N m^{-2}, vectors), and SST (°C, black contours at intervals of 0.4) anomalies along the equator (3°S–3°N) for (left) El Niño, (middle) La Niña, and (right) their sum. The SST anomalies are smoothed in the longitudinal direction with a 1–2–1 filter. Based on the SODA analysis and HadISST for 1958–2007.

basin cooling of the Indian Ocean during La Niña exert any influence on the Pacific?

The composite seasonal evolution of tropospheric temperature, surface wind, and precipitation anomalies along the equator for El Niño and La Niña are compared in Fig. 8 based on the NCEP–DOE reanalysis II and CMAP data for 1982–2008. Over the Pacific, tropospheric temperatures exhibit positive (negative) anomalies starting in May^0 concurrent with the underlying SST changes during El Niño (La Niña). Over the Indian Ocean, tropospheric temperature anomalies also follow closely the underlying SST anomalies. Tropospheric warming (cooling) occurs first over the western Indian Ocean in Jul^0–Aug^0 and starts to expand eastward in Oct^0–Nov^0 as the cooling (warming) off Sumatra weakens. During El Niño, this expansion of the tropospheric warming from the Indian Ocean to the Pacific induces anomalous surface easterly winds at its eastern edge, weakening the anomalous westerly winds between 110° and 160°W. During La Niña, the tropospheric cooling over the Indian Ocean also forces anomalous westerly winds at its eastern edge. However, the surface wind anomalies in the western Pacific are also influenced by the negative precipitation anomalies over the western half of the basin that induce easterly wind anomalies. Thus, the westerly wind anomalies forced by the Indian Ocean compete with the easterly anomalies induced by the Pacific rainfall anomalies.

We conjecture that the reason why the Pacific influence wins out over the Indian Ocean influence during La Niña but not during El Niño is that the Pacific precipitation anomalies are located farther west during La Niña compared to El Niño, which in turn is due to the nonlinear response of precipitation to SSTs (Fig. 9). Thus, the 10°–15° longitudinal shift of precipitation anomalies in the Pacific between El Niño and La Niña events seems to make a difference in the balance of local and remote wind forcing over the western Pacific. This zonal shift of the deep convection anomalies is also evident in the composite analysis of cloudiness anomalies based on shipboard observations from the International Comprehensive Ocean–Atmosphere Dataset (Woodruff et al. 2008) before the CMAP data period (not shown). The eastward displacement of precipitation anomalies during El Niño may also enable atmospheric circulation anomalies forced by negative SST and precipitation anomalies in the northwest tropical Pacific to affect the equatorial winds. Analysis of Indian Ocean SST anomalies for individual El Niño and La Niña events suggests that the Pacific events tend to decay more rapidly when the Indian Ocean SST anomalies

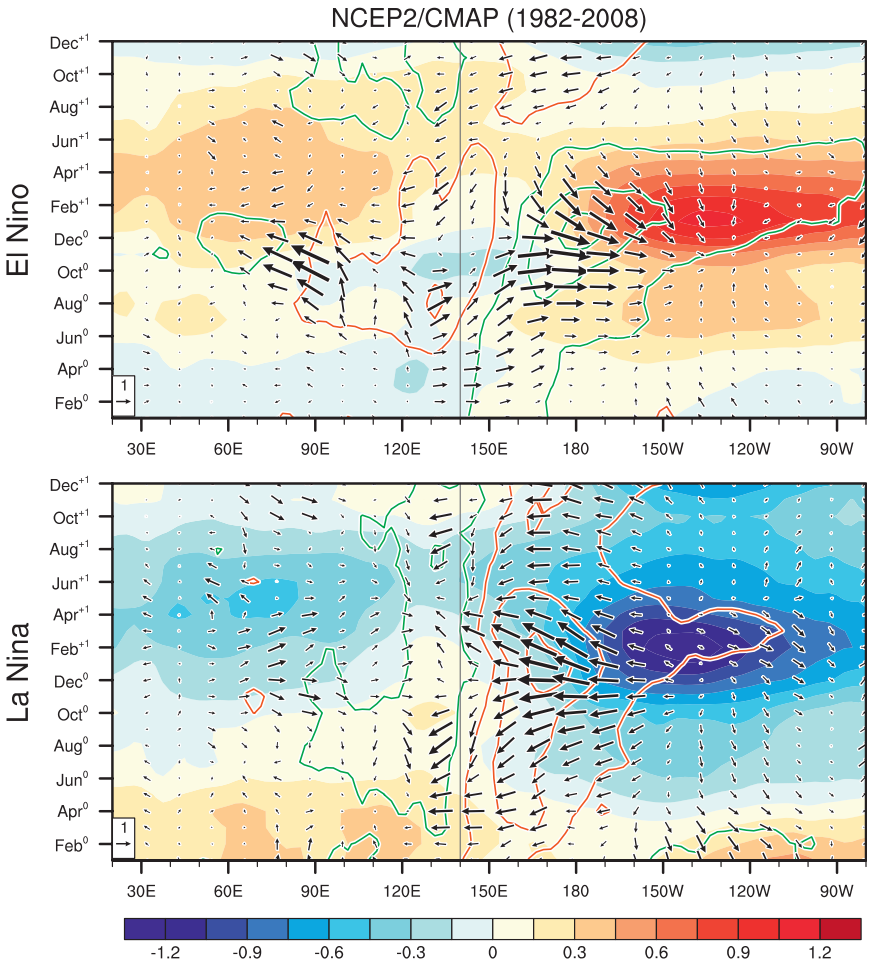

FIG. 8. Longitude–time sections of composite tropospheric temperature (°C, color shading), surface wind (m s^{-1}, vectors), and precipitation [mm day^{-1}, positive (negative) contours in green (orange) contours at ±1, 3, 5, . . .] anomalies along the equator (3°S–3°N) over the Pacific and Indian Oceans for (top) El Niño and (bottom) La Niña. The tropospheric temperatures are averaged between 850 and 250 hPa. The precipitation anomalies are smoothed in the longitudinal direction with a 1–2–1 filter. The gray vertical line at 140°E indicates the approximate location of the western end of the equatorial Pacific. Based on the NCEP–DOE reanalysis II and CMAP for 1982–2008.

are stronger and develop earlier (not shown). A recent study by Izumo et al. (2010) shows that ENSO forecasts can be significantly improved by including the state of the Indian Ocean SST anomalies in a simple statistical model. Finally, we suggest that the lack of a reversal in sign of the easterly wind anomalies in the western Pacific is responsible for the prolongation of La Niña into the next year. The return to normal conditions or transition to El Niño may be achieved via a buildup of the equatorial heat content due to slow oceanic adjustment (e.g., Jin 1997; Meinen and McPhaden 2000), as suggested by a gradual increase in the equatorially averaged sea surface height anomalies in the La Niña composite (Fig. 7) and individual multiyear La Niña events (not shown).

4. Summary

By analyzing a suite of ocean–atmosphere data for the past 27–109 yr, we have shown that there is a strong asymmetry in the duration of El Niño and La Niña. Both El Niño and La Niña typically begin in late spring–summer and intensify through the equatorial cold season. While most El Niños terminate rapidly after peaking toward the end of the year, many La Niñas persist through the following spring–summer and reintensify in winter; some even last through a third year and again strengthen during winter. The negative SST anomalies associated with La Niña propagate eastward during year 0, but the reintensified cooling near the end of year +1

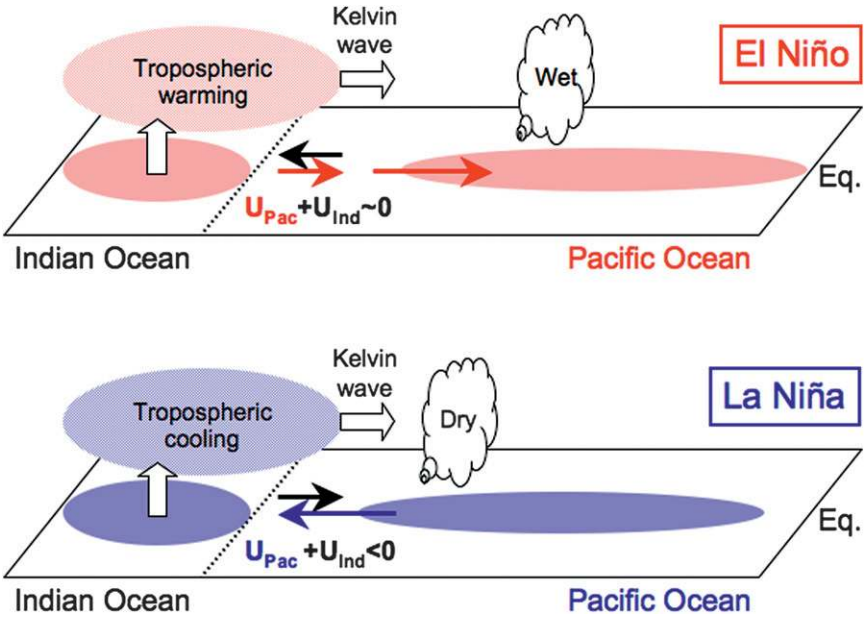

FIG. 9. Schematic diagram illustrating the hypothesized cause of the asymmetric wind response in the far western equatorial Pacific between (top) El Niño and (bottom) La Niña during the mature phase. Pink (blue) shaded ellipses depict positive (negative) SST anomalies over the Pacific and Indian Ocean during El Niño (La Niña). Red (blue) arrows indicate surface wind anomalies forced by Pacific SST anomalies during El Niño (La Niña); black arrows indicate surface wind anomalies forced by Indian Ocean SST anomalies. In the far western Pacific, the easterly (westerly) surface wind anomaly induced by the atmospheric Kelvin wave response to tropospheric heating (cooling) over the Indian Ocean balances (fails to balance) the westerly (easterly) surface wind anomaly forced by precipitation anomalies over the Pacific during El Niño (La Niña). The lack of balance of the surface wind anomalies over the far western Pacific during La Niña results from the westward shift of the Pacific precipitation anomaly because of the nonlinear dependence of atmospheric deep convection on the absolute SST. The net easterly surface wind anomaly over the far western Pacific during La Niña is hypothesized to prolong the event.

occurs simultaneously across the Pacific. Although this asymmetry in duration has been noted in a few recent studies, we demonstrate that it is a robust feature of ENSO variability throughout the past century.

The proposed mechanism for this asymmetric duration is summarized in a schematic diagram (Fig. 9). Because of the nonlinear response of atmospheric deep convection to SSTs, the center of the anomalous precipitation is displaced 10°–15° of longitude farther west during La Niña compared to El Niño. Through the developing and mature phases of La Niña, the suppressed atmospheric convection drives strong anomalous easterly winds over much of the western Pacific. El Niño exhibits a similar structure with reversed sign, except that a month prior to the mature phase, anomalous westerly winds begin to weaken in the far western Pacific. As suggested from previous studies, the delayed basin warming of the Indian Ocean increases tropospheric temperatures and forces a baroclinic atmospheric Kelvin wave into the western Pacific during El Niño. The easterly winds induced by this Kelvin wave weaken the anomalous westerly winds over the western Pacific. The same mechanism appears to work during La Niña, with the Kelvin wave forced by the basin cooling of the Indian Ocean inducing anomalous westerly winds at its eastern edge. However, the impact of local precipitation changes is so large that the anomalous equatorial winds remain easterly over the western Pacific. The enhanced duration of zonal wind anomalies in the western Pacific during La Niña compared to El Niño in turn leads to the prolongation of La Niña conditions into a second and sometimes even a third year. Preliminary analysis of atmospheric GCM experiments support this hypothesis, the results of which will be reported in a separate paper.

Our analysis focuses on strong El Niños and La Niñas for which the Niño-3.4 index exceeds one standard deviation at the mature phase (December). There is no apparent asymmetry in the duration of weaker warm and cold phases (see Fig. 1 for the Niño-3.4 time series for 1948–2008). During weaker warm phases, the equatorial

SST anomalies are often centered in the central Pacific and do not extend to the South American coast (Ashok et al. 2007; Kug et al. 2009; Kao and Yu 2009). Hoerling et al. (2001) also suggest that atmospheric deep convection responds linearly to moderate positive and negative SST anomalies. Thus, both the SST anomalies and the atmospheric deep convection response lack spatial asymmetry in weaker events. Warm events that do not develop until late summer–fall tend to be weaker and persist longer into the second year (Horii and Hanawa 2004). The late onset may delay and weaken the Indian Ocean SST response and hence the remote negative feedback to the western Pacific (Sooraj et al. 2009). The timing, pattern, and magnitude of SST anomalies in both the Pacific and Indian Oceans appear to be important factors controlling the persistence of individual El Niño and La Niña events, as well as intraseasonal variability that causes event to event differences (McPhaden 2008).

Coupled ocean–atmosphere models need to be examined for their ability to simulate not only the asymmetry in amplitude, but also the asymmetry in duration of the warm and cold phases of ENSO. A realistic simulation of the climatological rainbands in the tropical Pacific and ENSO-related SST anomalies in the Indian Ocean are a prerequisite. A cursory look at the 2000-yr control integration of the Geophysical Fluid Dynamics Laboratory Climate Model version 2.1 (GFDL CM2.1) indicates that this model exhibits asymmetry in the duration of El Niño and La Niña similar to what we have found in the observational record (Wittenberg 2009; see his Fig. 1) while a century-long control integration of the Community Climate System Model version 3 (Neale et al. 2008; Zhang et al. 2009) shows very weak ENSO asymmetry. Analysis of the Coupled Model Intercomparison Project phase 3 multimodel dataset by Ohba et al. (2010) indicates that the observed asymmetry in the duration of El Niño and La Niña is poorly simulated in most coupled GCM except in a few models including the GFDL CM2.1. Compared to the models that simulate the transition of El Niños to La Niñas after the mature phase, the models that simulate more persistent El Niños show equatorial Pacific precipitation anomalies displaced farther west because of the unrealistically strong climatological cold tongue. In these models, the basin warming of the Indian Ocean is also much weaker than in the models of high El Niño-to-La Niña transitivity. Ohba et al. (2010) argue that the westward shift of the Pacific precipitation anomalies allows equatorial wind anomalies to persist longer over the western Pacific, in agreement with our hypothesis. These results reaffirm the importance of realistic simulation of the mean climate for realistic simulation of ENSO. Long simulations of climate models that successfully simulate the observed ENSO asymmetries will provide an opportunity to assess how these aspects of ENSO may be modulated by climate change and variability with longer time scales.

Acknowledgments. Y. M. Okumura was supported through the NOAA Climate and Global Change Postdoctoral Fellowship and the funding for visiting scientists at the Climate and Global Dynamics Division of NCAR during the course of this study. The authors thank G. Vecchi, S.-P. Xie, S. Minobe, and M. Ohba for helpful discussion, J. M. Wallace and two anonymous reviewers for their constructive comments and suggestions, Y. Shen and J. Fasullo for their help in obtaining the ocean reanalysis data, and A. Phillips and D. Shea for technical assistance. The datasets used in this study were obtained online: the HadISST from the Met Office Hadley Centre (http://hadobs.metoffice.com/hadisst/), the OISST, NCEP reanalysis, NCEP–DOE reanalysis II, and CMAP from the NOAA/Earth System Research Laboratory Physical Science Division (http://www.esrl.noaa.gov/psd/data/gridded/), and the SODA analysis from the Asia–Pacific Data Research Center (http://apdrc.soest.hawaii.edu/).

REFERENCES

Alexander, M. A., I. Blade, M. Newman, J. R. Lanzante, N.-C. Lau, and J. D. Scott, 2002: The atmospheric bridge: The influence of ENSO teleconnections on air–sea interaction over the global oceans. *J. Climate,* **15,** 2205–2231.

——, D. J. Vimont, P. Chang, and J. D. Scott, 2010: The impact of extratropical atmospheric variability on ENSO: Testing the seasonal footprinting mechanism using coupled model experiments. *J. Climate,* **23,** 2885–2901.

Annamalai, H., S.-P. Xie, J. P. McCreary, and R. Murtugudde, 2005: Impact of Indian Ocean sea surface temperature on a developing El Niño. *J. Climate,* **18,** 302–319.

Ashok, K., S. K. Behera, S. A. Rao, H. Weng, and T. Yamagata, 2007: El Niño Modoki and its possible teleconnection. *J. Geophys. Res.,* **112,** C11007, doi:10.1029/2006JC003798.

Battisti, D. S., and A. C. Hirst, 1989: Interannual variability in a tropical atmosphere–ocean model—Influence of the basic state, ocean geometry, and nonlinearity. *J. Atmos. Sci.,* **46,** 1687–1712.

Bjerknes, J., 1969: Atmospheric teleconnections from the equatorial Pacific. *Mon. Wea. Rev.,* **97,** 163–172.

Boulanger, J.-P., S. Cravatte, and C. Menkes, 2003: Reflected and locally wind-forced interannual equatorial Kelvin waves in the western Pacific Ocean. *J. Geophys. Res.,* **108,** 3311, doi:10.1029/2002JC001760.

Burgers, G., and D. B. Stephenson, 1999: The ''normality'' of El Niño. *Geophys. Res. Lett.,* **26,** 1027–1030.

Carton, J. A., and B. S. Giese, 2008: A reanalysis of ocean climate using Simple Ocean Data Assimilation (SODA). *Mon. Wea. Rev.,* **136,** 2999–3017.

Chang, P., and Coauthors, 2006: Climate fluctuations of tropical coupled systems—The role of ocean dynamics. *J. Climate,* **19,** 5122–5174.

——, L. Zhang, R. Saravanan, D. J. Vimont, J. C. H. Chiang, L. Ji, H. Seidel, and M. K. Tippett, 2007: Pacific meridional mode and El Niño–Southern Oscillation. *Geophys. Res. Lett.,* **34,** L16608, doi:10.1029/2007GL030302.

Cole, J. E., J. T. Overpeck, and E. R. Cook, 2002: Multiyear La Niña events and persistent drought in the contiguous United States. *Geophys. Res. Lett.,* **29,** 1647, doi:10.1029/2007GL030302.

Delcroix, T., B. Dewitte, Y. duPenhoat, F. Masia, and J. Picaut, 2000: Equatorial waves and warm pool displacements during the 1992-1998 El Niño–Southern Oscillation events: Observation and modeling. *J. Geophys. Res.,* **105,** 26 045–26 062.

Deser, C., and J. M. Wallace, 1987: El Niño events and their relation to the Southern Oscillation: 1925–1986. *J. Geophys. Res.,* **92,** 14 189–14 196.

——, and ——, 1990: Large-scale atmospheric circulation features of warm and cold episodes in the tropical Pacific. *J. Climate,* **3,** 1254–1281.

Fedorov, A. V., and S. G. Philander, 2000: Is El Niño changing? *Science,* **288,** 1997–2002.

Harrison, D. E., and G. A. Vecchi, 1999: On the termination of El Niño. *Geophys. Res. Lett.,* **26,** 1593–1596.

Hoerling, M. P., and A. Kumar, 2003: The perfect ocean for drought. *Science,* **299,** 691–694.

——, ——, and M. Zhong, 1997: El Niño, La Niña, and the nonlinearity of their teleconnections. *J. Climate,* **10,** 1769–1786.

——, ——, and T. Xu, 2001: Robustness of the nonlinear climate response to ENSO's extreme phases. *J. Climate,* **14,** 1277–1293.

Horii, T., and K. Hanawa, 2004: A relationship between timing of El Niño onset and subsequent evolution. *Geophys. Res. Lett.,* **31,** L06304, doi:10.1029/2003gl019239.

Izumo, T., and Coauthors, 2010: Influence of the state of the Indian Ocean dipole on the following year's El Niño. *Nat. Geosci.,* **3,** 168–172.

Jin, F.-F., 1997: An equatorial ocean recharge paradigm for ENSO. Part I: Conceptual model. *J. Atmos. Sci.,* **54,** 811–829.

——, S.-I. An, A. Timmermann, and J. Zhao, 2003: Strong El Niño events and nonlinear dynamical heating. *Geophys. Res. Lett.,* **30,** 1120, doi:10.1029/2002GL016356.

Kalnay, E., and Coauthors, 1996: The NCEP/NCAR 40-Year Reanalysis Project. *Bull. Amer. Meteor. Soc.,* **77,** 437–471.

Kanamitsu, M., W. Ebisuzaki, J. Woollen, S.-K. Yang, J. J. Hnilo, M. Fiorino, and G. L. Potter, 2002: NCEP-DOE AMIP-II Reanalysis (R-2). *Bull. Amer. Meteor. Soc.,* **83,** 1631–1643.

Kang, I.-S., and J.-S. Kug, 2002: El Niño and La Niña sea surface temperature anomalies: Asymmetry characteristics associated with their wind stress anomalies. *J. Geophys. Res.,* **107,** 4372, doi:10.1029/2001JD000393.

Kao, H.-Y., and J.-Y. Yu, 2009: Contrasting eastern Pacific and central Pacific types of ENSO. *J. Climate,* **22,** 615–632.

Kerr, R. A., 1988: La Niña's big chill replaces El Niño. *Science,* **241,** 1037–1038.

Kessler, W. S., 2002: Is ENSO a cycle or a series of events? *Geophys. Res. Lett.,* **29,** 2125, doi:10.1029/2002GL015924.

Klein, S. A., B. J. Soden, and N.-C. Lau, 1999: Remote sea surface temperature variations during ENSO: Evidence for a tropical atmospheric bridge. *J. Climate,* **12,** 917–932.

Kug, J.-S., and I.-S. Kang, 2006: Interactive feedback between ENSO and the Indian Ocean. *J. Climate,* **19,** 1784–1801.

——, F.-F. Jin, and S.-I. An, 2009: Two types of El Niño events: Cold tongue El Niño and warm pool El Niño. *J. Climate,* **22,** 1499–1515.

Larkin, N. K., and D. E. Harrison, 2002: ENSO warm (El Niño) and cold (La Niña) event life cycles: Ocean surface anomaly patterns, their symmetries, asymmetries, and implications. *J. Climate,* **15,** 1118–1140.

Lau, K.-M., 1985: Elements of a stochastic-dynamical theory of the long-term variability of the El Niño–Southern Oscillation. *J. Atmos. Sci.,* **42,** 1552–1558.

McPhaden, M. J., 2008: Evolution of the 2006-2007 El Niño: The role of intraseasonal to interannual time scale dynamics. *Adv. Geosci.,* **14,** 219–230.

——, and X. Yu, 1999: Equatorial waves and the 1997-98 El Niño. *Geophys. Res. Lett.,* **26,** 2961–2964.

——, and X. Zhang, 2009: Asymmetry in zonal phase propagation of ENSO sea surface temperature anomalies. *Geophys. Res. Lett.,* **36,** L13703, doi:10.1029/2009GL038774.

Meinen, C. S., and M. J. McPhaden, 2000: Observations of warm water volume changes in the equatorial Pacific and their relationship to El Niño and La Niña. *J. Climate,* **13,** 3551–3559.

Mitchell, T. P., and J. M. Wallace, 1992: The annual cycle in equatorial convection and sea surface temperature. *J. Climate,* **5,** 1140–1156.

Nagura, M., K. Ando, and K. Mizuno, 2008: Pausing of the ENSO cycle: A case study from 1998 to 2002. *J. Climate,* **21,** 342–363.

Neale, R. B., J. H. Richter, and M. Jochum, 2008: The impact of convection on ENSO: From a delayed oscillator to a series of events. *J. Climate,* **21,** 5904–5924.

Neelin, J. D., D. S. Battisti, A. C. Hirst, F.-F. Jin, Y. Wakata, T. Yamagata, and S. E. Zebiak, 1998: ENSO theory. *J. Geophys. Res.,* **103,** 14 261–14 290.

Ohba, M., and H. Ueda, 2007: An impact of SST anomalies in the Indian Ocean in acceleration of the El Niño to La Niña transition. *J. Meteor. Soc. Japan,* **85,** 335–348.

——, and ——, 2009: Role of nonlinear atmospheric response to SST on the asymmetric transition process of ENSO. *J. Climate,* **22,** 177–192.

——, D. Nohara, and H. Ueda, 2010: Simulation of asymmetric ENSO transition in the WCRP CMIP3 multimodel experiments. *J. Climate,* in press.

Okumura, Y., and S.-P. Xie, 2006: Some overlooked features of tropical Atlantic climate leading to a new Niño-like phenomenon. *J. Climate,* **19,** 5859–5874.

Penland, C., and P. D. Sardeshmukh, 1995: The optimal growth of tropical sea surface temperature anomalies. *J. Climate,* **8,** 1999–2024.

Philander, S. G. H., 1985: El Niño and La Niña. *J. Atmos. Sci.,* **42,** 2652–2662.

Picaut, J., F. Masia, and Y. duPenhoat, 1997: An advective-reflective conceptual model for the oscillatory nature of the ENSO. *Science,* **277,** 663–666.

——, E. Hackert, A. J. Busalacchi, R. Murtugudde, and G. S. E. Lagerloef, 2002: Mechanisms of the 1997-1998 El Niño–La Niña, as inferred from space-based observations. *J. Geophys. Res.,* **107,** 3037, doi:10.1029/2001JC000850.

Rasmusson, E. M., and T. H. Carpenter, 1982: Variations in tropical sea surface temperature and surface wind fields associated with the Southern Oscillation/El Niño. *Mon. Wea. Rev.,* **110,** 354–384.

Rayner, N. A., D. E. Parker, E. B. Horton, C. K. Folland, L. V. Alexander, D. P. Rowell, E. C. Kent, and A. Kaplan, 2003: Global analyses of sea surface temperature, sea ice, and night marine air temperature since the late nineteenth century. *J. Geophys. Res.,* **108,** 4407, doi:10.1029/2002JD002670.

Reynolds, R. W., N. A. Rayner, T. M. Smith, D. C. Stokes, and W. Q. Wang, 2002: An improved in situ and satellite SST analysis for climate. *J. Climate,* **15,** 1609–1625.

Ropelewski, C. F., and M. S. Halpert, 1989: Precipitation patterns associated with the high index phase of the Southern Oscillation. *J. Climate,* **2,** 268–284.

Schopf, P. S., and M. J. Suarez, 1988: Vacillations in a coupled ocean–atmosphere model. *J. Atmos. Sci.,* **45,** 549–566.

——, and R. J. Burgman, 2006: A simple mechanism for ENSO residuals and asymmetry. *J. Climate,* **19,** 3167–3179.

Schott, F. A., S.-P. Xie, and J. P. McCreary, 2009: Indian Ocean circulation and climate variability. *Rev. Geophys.,* **47,** RG1002, doi:10.1029/2007RG000245.

Sooraj, K. P., J.-S. Kug, T. Li, and I.-S. Kang, 2009: Impact of El Niño onset timing on the Indian Ocean: Pacific coupling and subsequent El Niño evolution. *Theor. Appl. Climatol.,* **97,** 17–27.

Thompson, C. J., and D. S. Battisti, 2001: A linear stochastic dynamical model of ENSO. Part II: Analysis. *J. Climate,* **14,** 445–466.

Tokinaga, H., and Y. Tanimoto, 2004: Seasonal transition of SST anomalies in the tropical Indian Ocean during El Niño and Indian Ocean dipole years. *J. Meteor. Soc. Japan,* **82,** 1007–1018.

Trenberth, K. E., 1997: The definition of El Niño. *Bull. Amer. Meteor. Soc.,* **78,** 2771–2777.

——, G. W. Branstator, D. Karoly, A. Kumar, N.-C. Lau, and C. Ropelewski, 1998: Progress during TOGA in understanding and modeling global teleconnections associated with tropical sea surface temperatures. *J. Geophys. Res.,* **103,** 14 291–14 324.

——, J. M. Caron, D. P. Stepaniak, and S. Worley, 2002: Evolution of El Niño–Southern Oscillation and global atmospheric surface temperatures. *J. Geophys. Res.,* **107,** 4065, doi:10.1029/2000JD000298.

Tziperman, E., S. E. Zebiak, and M. A. Cane, 1997: Mechanisms of seasonal–ENSO interaction. *J. Atmos. Sci.,* **54,** 61–71.

Vecchi, G. A., 2006: The termination of the 1997/98 El Niño. Part II: Mechanisms of atmospheric change. *J. Climate,* **19,** 2647–2664.

Wang, B., and S.-I. An, 2002: A mechanism for decadal changes of ENSO behavior: Roles of background wind changes. *Climate Dyn.,* **18,** 475–486.

Wang, C., and J. Picaut, 2004: Understanding ENSO physics—A review. *Earth's Climate: The Ocean–Atmosphere Interaction, Geophys. Monogr.,* Vol. 147, Amer. Geophys. Union, 21–48.

Watanabe, M., and F.-F. Jin, 2002: Role of Indian Ocean warming in the development of Philippine Sea anticyclone during ENSO. *Geophys. Res. Lett.,* **29,** 1478, doi:10.1029/2001GL014318.

Weisberg, R. H., and C. Wang, 1997: A western Pacific oscillator paradigm for the El Niño–Southern Oscillation. *Geophys. Res. Lett.,* **24,** 779–782.

Wittenberg, A. T., 2009: Are historical records sufficient to constrain ENSO simulations? *Geophys. Res. Lett.,* **36,** L12702, doi:10.1029/2009GL038710.

Woodruff, S. D., H. F. Diaz, E. C. Kent, R. W. Reynolds, and S. J. Worley, 2008: The evolving SST record from ICOADS. *Climate Variability and Extremes during the Past 100 Years,* S. Brönnimann et al., Eds., Vol. 33, *Advances in Global Change Research,* Springer, 65–83.

Wu, R., and S.-P. Xie, 2003: On equatorial Pacific surface wind changes around 1977: NCEP–NCAR reanalysis versus COADS observations. *J. Climate,* **16,** 167–173.

Xie, P., and P. A. Arkin, 1996: Analyses of global monthly precipitation using gauge observations, satellite estimates, and numerical model predictions. *J. Climate,* **9,** 840–858.

Xie, S.-P., 1994: On the genesis of the equatorial annual cycle. *J. Climate,* **7,** 2008–2013.

——, 1995: Interaction between the annual and interannual variations in the equatorial Pacific. *J. Phys. Oceanogr.,* **25,** 1930–1941.

——, H. Annamalai, F. A. Schott, and J. P. McCreary, 2002: Structure and mechanisms of South Indian Ocean climate variability. *J. Climate,* **15,** 864–878.

——, K. Hu, J. Hafner, H. Tokinaga, Y. Du, G. Huang, and T. Sampe, 2009: Indian Ocean capacitor effect on Indo-Western Pacific climate during the summer following El Niño. *J. Climate,* **22,** 730–747.

Yoo, S.-H., J. Fasullo, S. Yang, and C.-H. Ho, 2010: On the relaionship between Indian Ocean sea surface temperature and the transition from El Niño to La Niña. *J. Geophys. Res.,* **115,** D15114, doi:10.1029/2009JD012978.

Zhang, T., D.-Z. Sun, R. Neale, and P. J. Rasch, 2009: An evaluation of ENSO asymmetry in the Community Climate System Models: A view from the subsurface. *J. Climate,* **22,** 5933–5961.

Zhang, X., and M. J. McPhaden, 2006: Wind stress variations and interannual sea surface temperature anomalies in the eastern equatorial Pacific. *J. Climate,* **19,** 226–241.

——, and ——, 2008: Eastern equatorial Pacific forcing of ENSO sea surface temperature anomalies. *J. Climate,* **21,** 6070–6079.